

# Temporal-Harmonic Specific POD Mode Extraction

Gilead Tadmor\* and Daniel Bissex†

*Electrical & Computer Engineering, 440 DA, Northeastern University  
Boston, MA 02115, USA*

Bernd R. Noack‡

*Inst. of Fluid Mechanics and Technical Acoustics  
Berlin University of Technology,  
Straße des 17. Juni, 10623 Berlin, Germany*

Marek Morzyński§

*Institute of Combustion Engines and Transportation,  
Poznan University of Technology,  
Piotrowo 3, 60-965 Poznan, Poland*

Tim Colonius¶ and Kunihiko Taira||

*Engineering and Applied Science,  
California Institute of Technology,*

*1200 East California Boulevard, MS 104-44 Pasadena, CA 91125, USA*

While POD / PCA / KL approximations are statistically energetically optimal, statistical optimality is indeed the sole consideration these (equivalent) methods invoke. This type of approximation is neither geared for, nor is it optimized to extract modes based on their significance to an underlying system dynamics. Furthermore, as computational considerations limit the size of empirical ensembles used for mode extraction, the resulting mode set is significantly effected by the arbitrariness of the ensemble selection. System theoretic model reductions methods aim to home on dynamically significant modes by direct interrogation of the underlying equation, such as the linearized Navier-Stokes equations. An alternative / complimentary approach is to impose a priori knowledge of structural properties, such as symmetry and periodicity, on the mode-extraction procedure. The idea is that these conditions will force the selection of physically meaningful modes, and thus enables an effective appeal to first principles. Here we focus on systems known to be periodically dominant, and describe a simple method to extract modes associated with temporal harmonics. The method accommodates time variations in the dominant frequency(ies) and exploits a preliminary data compression, such as by the standard POD procedure.

## I. Overview

The Proper Orthogonal Decomposition (POD) approximation algorithm<sup>1-3</sup> is an optimally efficient subspace approximation of the fluctuations in a data ensemble, under dimensionality bounds. It is therefore extremely appealing in the context of mode selection for a Galerkin model reduction of complex, distributed nonlinear systems, such as those involving fluid flow. It is, however, an intrinsically statistical method that

---

\*Professor, ECE and Mathematics, Northeastern University, Boston, MA 02115, Senior Member, AIAA.

†Graduate Student, ECE, 440 DA, Northeastern University, Boston, MA 02115

‡Ass. Professor, Institute of Fluid Mechanics and Technical Acoustics, Berlin University of Technology, Berlin, Germany.

§Professor, Inst. of Combustion Engines and Transportation, Poznan University of Technology, Poland

¶Professor, Mechanical Engineering, Caltech, Pasadena, CA 91125, AIAA Member

||Graduate Student, Mechanical Engineering, Caltech, Pasadena, CA 91125

does not take into consideration even the temporal order of the data snapshots it uses, let alone any consideration of dynamics. While it is intuitively reasonable to assume that the most energetic modes will play a dominant dynamic role, evidence of difficulties to reach ample dynamic representation abound when it comes to very low order models, such as those used for feedback flow control design and implementation.

One common POD pitfall is manifest in the analysis of transient trajectories, traversing changes in the operating conditions. The benchmark of a flat plate at time varying angle of attack that is used in our paper is a case in point. As the angle of attack changes the systems mean field changes significantly, as does the leading shedding harmonic<sup>4</sup>, once the flow separates. In such cases it is common that all but the time dynamics of all but the most dominant mode pair will capture harmonically rich time dynamics, reflecting a spatial mix of multiple vortical structures and wave lengths. Arguably, when it comes to very low order models, it is desirable, rather, that modes will represent physically distinct flow structures. A focus on a globally synchronized instantaneous set of vortical structures that are associated with similar spatial and temporal frequencies, are example. The use of such modes then allows the model to represent the temporal dynamics at the characteristic frequencies, associated with the said structures. In contrast, when each mode represents multiple temporal frequencies, a truncated model will be incapable to properly represent them.

A *top-down* approach to address such difficulties is the direct appeal to the governing equation, such as by using balanced truncation model reduction<sup>5-8</sup>, applied to the linearized distributed system. Such system theoretic tools are geared to reveal, e.g., internal and less energetic modes that act as essential dynamic catalysts but are not conspicuous from a spatially global energy consideration. This approach too may suffer from some potential shortcomings, chief among which is the reliance on a linearized model. This may exclude nonlinear interactions, such as the interactions of fluctuations with the mean flow that can be essential for global dynamic representation<sup>9,10</sup>, but which might not be observed by an inherently local, linearized model. Even in those case where a balanced model reduction is an appropriate approach, a key feature of the methods cited above<sup>5-8</sup> is that time coefficients of dominant empirical modes and a POD or POD-like approximation make a natural choice of the observable outputs used for the reduction. In that case two it is advantageous to select those modes in a way that will reflect clear coherent physical structures.

That is the purpose of this note. In this abstract we shall focus on a brief review of the mode extraction procedure, illustrated by the example of the transient flow over a two dimensional flat plate at a time varying angle of attack. The full paper will include the analysis of the much more complex three dimensional case, along with mean-field Galerkin modelin the spirit of<sup>9,10</sup>, representing the dynamic interactions of the slowly time varying mean field and the fast oscillating fluctuations.

## II. The Transient Flow Over a Flat Plate

The algorithm is demonstrated in an analysis of simulation data for a flat plate in two and three dimensions. The immersed boundary condition simulation code is described in.<sup>11</sup> In this preliminary abstract we focus on the two dimensional case at the Reynolds number  $Re = 300$ , using  $62k$  grid points. The simulation is conducted using a time step of  $dt = .01$  CTU (convective time units), with snapshots saved every 10 time steps. The trajectory analyzed here reflects 200 CTUs, captured by 2000 snapshots. To create a characteristic change of flow within the simulation, the plate is raised to a horizontal position, held, and then lowered back to its orginal position of  $AOA = 30^\circ$ . The POD analysis must thus handle the complex dynamics when the plates AOA passes through the bifurcation point at which the flow sheds the vortex street. Periodic vortex shedding again resumes when the AOA again passes though the bifurcation point as it returns to its start position. The green recta-linear line in the plots in Figure 1 represents the time dependence of the AOA. The reference trajectory was analyzed by both the standard POD algorithm and a fast, approximate POD algorithm described in the companion paper,<sup>12</sup> with a required average resolution of 99% of the fluctuation energy. The first 30 of the 34 required POD modes, that are yielded by the two methods are essentially identical. The POD eigenvalues of the two methods are depicted in Figure 1. That figure also include an examples comparing the POD / approximate POD analysis of the entire data trajectory, with analysis of short time segments, along that trajectory. In particular, the figure illustrates the dependence of the resolution on the number of expansion modes used.

While the dominant POD mode pair is indeed nearly harmonically pure, other POD modes of that simulation tend to mix the influence of multiple spatial wave lengths and temporal frequencies. Examples of this phenomenon are depicted in Figure 2.

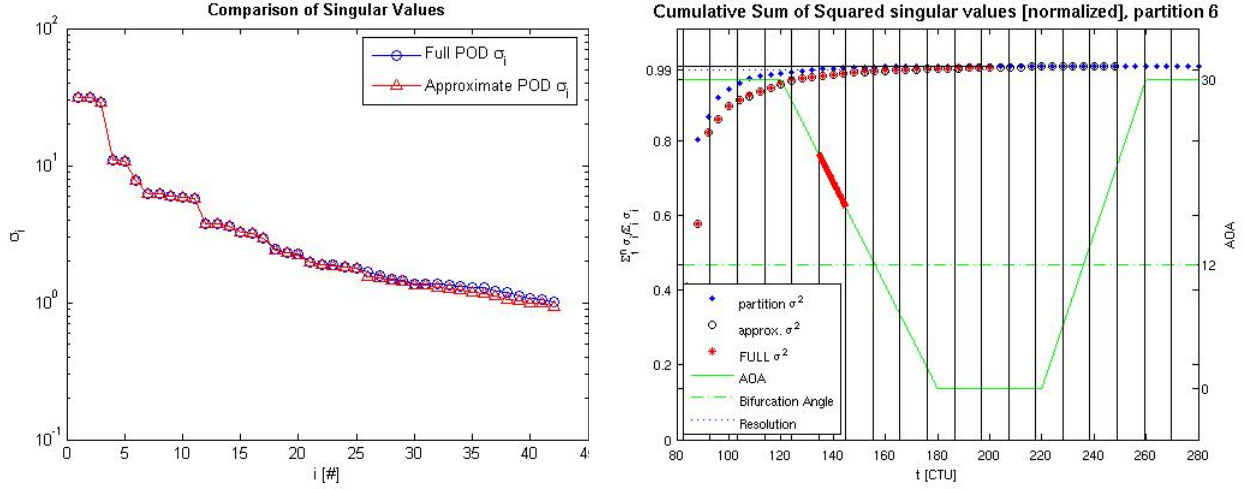


Figure 1. Left Singular values of the actual and approximate POD. Right: Comparisons of the TKE resolution as a function of the number of modes used in a global POD approximation (red stars), modes from a global approximate POD computations (circles), and the local resolution of a short time intervals, using POD analysis of these intervals (blue dots). The red segment indicates the respective interval. The recta-linear green line indicates the AOA as a time function. The horizontal axis indicates time

### III. Extraction of Harmonically Pure Modes

The algorithm is based on a separation of the data trajectory by temporal filtering as the sum of several, harmonically clean - single frequency trajectories, followed by an independent POD analysis of each of these trajectories. Two obvious hurdles need to be addressed by this program:

- The time variation in the instantaneous frequency.
- The high computational burden of temporal filtering a very high dimensional trajectory.

The second hurdle was addressed by performing a preliminary high resolution POD (or using the fast POD approximation of<sup>12</sup>) as a data compression, rather than a tool for the final mode extraction. As mentioned above, an averaged 99% TKE resolution is achievable by a compression to a 34 dimensional space. Following this step, dimensionality and computational complexity cease to be a matter of any significance. The remainder of this section outlines the other aspects of the algorithm. For later use we denote the compression by

$$\mathbf{u}(\mathbf{x}, t) \approx \mathbf{u}_0(\mathbf{x}) + \sum_{k=1}^N a_k(t) \mathbf{u}_k(\mathbf{x}) = \mathbf{u}_0(\mathbf{x}) + \mathbf{U}(\mathbf{x}) \mathbf{a}(t) \quad (1)$$

where  $\mathbf{x} = (x, y)$  indicates position with the standard Euclidean coordinates,  $\mathbf{u} = (u, v)$  indicates the velocity field and its stream-wise and transverse components,  $\mathbf{u}_i$  are the expansion modes and  $\mathbf{a} = (a_1, \dots, a_N)$  is the corresponding vector of time coefficients. Henceforth the vector  $\mathbf{a}(t) \in \mathfrak{R}^N$  isometrically represents the compressed velocity field.

#### A. The instantaneous frequency, period and phase

There are a variety of conceivable methods to estimate the instantaneous frequency of a harmonically dominant signal<sup>13,14</sup>. Following are some obvious options for the signals with relatively fast variations in the dominant frequency, all based on an analysis of the signal over a moving time window  $[t - 0.5T, t + 0.5T]$ :

1. Applying the FFT algorithm to the signal segment over the moving window and selecting the frequency of the amplitude peak. The disadvantage of this approach is that it requires a relatively high sampling rate.

2. Searching for the maximal resolution by a truncated Fourier expansions over a bank of candidate frequencies. Note that here the fixed interval length of  $T$  will generally *not* be a full period, for the considered candidate frequencies. This deficiency is addressed by the use of oblique projections.
3. Enriching the harmonic base functions in the previous option with a linear base function, to account for rapid change in period means.

In any of these options, low pass filtering of either the frequency or the associated period is likely to be necessary to smooth out step changes due to quantization of the considered filter-bank or the FFT.

Here we opted for a simpler and fairly robust option that is available in typical periodically dominant flows. Namely, notwithstanding the blending of multiple frequencies in higher modes, the most dominant mode pair, say  $\mathbf{u}_i$ ,  $i = 1, 2$  typically represents a fairly clean amplitude modulated oscillation frequency. This is indeed the situation in the two dimensional flow over a stalled flat plate. In that case the time coefficients will be of the form

$$a_1(t) = A_1(t) \cos(\phi(t)) \text{ and } a_2(t) = A_2(t) \sin(\phi(t))$$

where both  $A(t)$  and  $\omega(t) = \dot{\phi}(t)$  vary at a sufficiently longer time constant than the instantaneous period  $T(t) = 2\pi/\omega(t)$ . In that case an instantaneous concept of the phase can be extracted as

$$\phi(t) = \angle(a_1(t) + i a_2(t))$$

This signal can be low pass-filtered and its time derivative can be well estimated by the slope of a linear approximation over a moving window. During those time intervals where crossed the bifurcation point into the stable-attached regime, the frequency is estimated - merely as a matter of completeness - by linear interpolation between points where it is well defined.

## B. Harmonic partition of the data trajectory

The unwrapped phase trajectory  $\phi(t)$  is generically a monotonous function of time. Substituting time by this phase signal as the argument of time trajectories, simplifies the definition of frequency which becomes identically equal to  $\omega \equiv 1$ . Since the data trajectory is now represented by the compressed signal  $\mathbf{a}(t) \in \mathbb{R}^N$ , it is numerically inexpensive to use an interpolation scheme to resample  $\mathbf{a}$  at equal phase increments and redefine it as a function of the phase  $\phi$ .

Truncated harmonic expansion of the (sampled)  $\mathbf{a}(\phi)$  over a moving window  $[\phi - \pi, \phi + \pi]$  are easily computed, as

$$\mathbf{a}(\phi + \psi) \approx \mathbf{a}^0(\phi) + \sum_{k=1}^K \mathbf{a}^k(\phi) \cos(k\psi) + \mathbf{b}^k(\phi) \sin(k\psi), \quad \psi \in [-\pi, \pi]$$

Mid-interval evaluation, at  $\psi = 0$  then yields

$$\mathbf{a}(\phi) \approx \mathbf{a}^0(\phi) + \sum_{k=1}^K \mathbf{a}^k(\phi)$$

Noting that, by definition and the and the postulated existence of a harmonic partition, following a small phase increment one has

$$\mathbf{a}^k(\phi + \Delta\phi) \approx \mathbf{a}^k(\phi) \cos(k\Delta\phi) + \mathbf{b}^k(\phi) \sin(k\Delta\phi)$$

meaning that  $\mathbf{a}^k(\phi)$  represents the oscillatory component of  $\mathbf{a}(\phi)$  at the  $k^{th}$  harmonic.

One shortcoming of this procedure - essentially an IIR band filtering of  $\mathbf{a}(\phi)$  - is that the partition comes with no a priori guarantee of spatial orthogonality. That is we might have  $\mathbf{a}^k(\phi) \not\perp \mathbf{a}^\ell(\phi)$ . Nonetheless, it is noted that temporal frequencies are generically tightly coupled with spatial wave lengths of vortical structures and that velocity fields at different wave length are well expected to be nearly orthogonal. In particular, the correlation matrix of the harmonic partitioning  $C(t) = [C_{k\ell}(\phi)] = [\mathbf{a}^k(\phi)' \mathbf{a}^\ell(\phi)]$  is strongly diagonally dominant as long as the partition is in term of truly dominant frequencies, associated with distinct coherent spatial structures. That is indeed the case in the flat plate benchmark, when the zero (base flow) and first harmonic components are used.

### C. Harmonically Clean Mode Extraction

The next step is to apply the POD algorithm separately to each of the “pure harmonic” data trajectories  $\mathbf{a}^k(\phi)$ . The modes obtained this way are vectors  $\mathbf{q}_i^k \in \mathfrak{R}^N$ . Each of the corresponds, isometrically to a fluctuation vector field, or mode, over the original domain, when interpreted as the coefficient vector in the Galerkin approximation (1). Again, the combined collection of modes obtained this way is not guaranteed to be orthogonal. Yet as long as the data used is not noise dominated and corresponds to existing coherent structures, its correlation matrix is expected to be diagonally dominated and close to the identity. This enables a numerically sound oblique projection in a non-orthogonal Galerkin approximation, akin to (1). Example of a harmonically clean modes obtained via this procedure, and of its time coefficient, are provided in Figure 3

Table 1 provides the singular values are of the covariance matrix  $\bar{\Psi}'_\gamma \bar{\Psi}_\gamma$ , where  $\bar{\Psi}$  represents the truncated collection of the  $0^{th}$ ,  $1^{st}$  and  $2^{nd}$  harmonic sets found by the harmonic partitioning algorithm. The deviation of the singular values from unity and their condition numbers are indicators of the non-orthogonality of the obtained basis. Truncation is performed using the resolution bound  $0 < \gamma < 1$ , in an exactly equivalent manner to the truncation of the original singular matrices of the POD algorithm performed by the resolution bound  $\lambda$ . Orthogonality improves as fewer harmonically partitioned modes are retained.

Range of singular values of $\bar{\Psi}'_\gamma \bar{\Psi}_\gamma$			
<b>17 modes, <math>\gamma = 0.95</math></b>	<b>12 modes, <math>\gamma = 0.90</math></b>	<b>9 modes, <math>\gamma = 0.85</math></b>	<b>7 modes, <math>\gamma = 0.80</math></b>
$0.026 \leq \sigma_i \leq 1.98$	$0.303 \leq \sigma_i \leq 1.7$	$.346 \leq \sigma_i \leq 1.35$	$0.958 \leq \sigma_i \leq 1.65$

Table 1. Ranges of singular values for the covariance of the cleaned modes.

## IV. What Next

The complete paper will include the following additional components.

### A. Mode deformation and local mode sets

The deformation of dominant coherent structures is a well known phenomenon that bars the use of a very low order model, optimized in one operating condition, in another operating condition. In<sup>15</sup> we introduced the concept of mode interpolation as a means to maintain the low dimensionality of the Galerkin system of differential equations without losing the quality of the representation. The idea was to use a fix number of modes and allow these mode to deform, as the system traverses different operating conditions. In certain cases, such as the change of AOA, it is expected that this will result in a parameterized set of modes that could be computed as interpolants of few globally computed modes. The paper<sup>16</sup> provide one mode interpolation scheme. The current discussion leads to an alternative endowed with the added advantage of using harmonically cleaned structures. Specifically, as described earlier, the  $k^{th}$  harmonic trajectory can be globally approximated as

$$\mathbf{a}^k(t) \approx \sum_{\ell=1}^{L(k)} d_i^k(t) \mathbf{q}_i^k = \mathbf{Q}^k \mathbf{d}^k(t)$$

Once again, the mapping  $\mathbf{d}^k \mapsto \mathbf{a}^k : \mathfrak{R}^{L(k)} \mapsto \mathfrak{R}^N$  is an isometry. Applying POD analysis of the trajectory  $\mathbf{d}^k(t)$  over a moving time window whose length may represent few period of the main harmonic may isolate far fewer modes - ideally, a single mode pair if  $k \geq 1$  and a single mode if  $k = 0$  - that dominate the flow over that window. The local mode(s) will be a combination of the original modes  $\mathbf{q}_i^k$ , with operating-condition-dependent coefficients. An indicator of the parametrization of the deformable local modes would typically be extracted from flow measurements.<sup>15</sup>

### B. Mean Field Models

Mean field models have been developed as enablers for very low order flow models<sup>9,10</sup> (see also, e.g.<sup>17-20</sup>). Conceptually, these models couple an algebraic or slowly varying dynamic version of Reynolds' equation

with a pure harmonic counterpart, at the dominant frequency. This coupling is an enabler for modeling the interactions between the time varying mean field and the fluctuation, and their critical effect on both the destabilization of the steady solution and the stabilization of natural and controlled attractors. We shall use develop an interpolated mean field model, governing the dynamics of the local modes obtained as described above.

## References

- <sup>1</sup>Sirovich, L., “Turbulence and the dynamics of coherent structures, Parts I–III,” *Quart. Appl. Math.*, Vol. XLV, 1987, pp. 561–590.
- <sup>2</sup>Holmes, P., Lumley, J., and Berkooz, G., *Turbulence, Coherent Structures, Dynamical Systems and Symmetry*, Cambridge University Press, Cambridge, 1998.
- <sup>3</sup>Smith, T. R., Moehlis, J., and Holmes, P., “Low-Dimensional Modelling of Turbulence Using the Proper Orthogonal Decomposition: A Tutorial,” *Nonlinear Dynamics*, Vol. 41, 2005, pp. 275 – 307.
- <sup>4</sup>Mittal, R., Kotapati, R. B., and Cattafesta, L., “Numerical Study of Resonant Interactions and Flow Control in a Canonical Separated Flow,” *43rd AIAA Aerospace Sciences Meeting and Exhibit*, 2005, AIAA Paper 2005-1261.
- <sup>5</sup>Lall, S., Marsden, J. E., and Glavaski, S., “A subspace approach to balanced truncation for model reduction of nonlinear control systems,” *International Journal on Robust and Nonlinear Control*, Vol. 12, 2002, pp. 519–535.
- <sup>6</sup>Willcox, K. and Peraire, J., “Balanced Model Reduction via the Proper Orthogonal Decomposition,” *AIAA JOURNAL*, Vol. 40, 2000, pp. 2323–2330.
- <sup>7</sup>Rowley, C., “Model reduction for fluids, using balanced proper orthogonal decomposition,” *Int. J. on Bifurcation and Chaos*, Vol. 15, 2005, pp. 997–1013.
- <sup>8</sup>Ma, Z., Rowley, C. W., and Tadmor, G., “Snapshot-based Balanced Truncation for Linear Time-periodic Systems,” *IEEE Trans. Autom. Control*, 2007, submitted.
- <sup>9</sup>Noack, B., Afanasiev, K., Morzyński, M., Tadmor, G., and Thiele, F., “A hierarchy of low-dimensional models for the transient and post-transient cylinder wake,” *J. Fluid Mech.*, Vol. 497, 2003, pp. 335–363.
- <sup>10</sup>Luchtenburg, M., Günther, B., King, R., and Tadmor, G., “A generalised mean-field model of the natural and high-frequency actuated flow around a high-lift configuration,” *J. Fluid Mech.*, 2007, sbmitted.
- <sup>11</sup>Taira, K., Dickson, W., Colonius, T., Dickinson, M., and Rowley, C., “Unsteadiness in Flow over a Flat Plate at Angle-of-Attack at Low Reynolds Numbers,” *45th AIAA Aerospace Sciences Meeting and Exhibit*, 2007, AIAA Paper 2007-710.
- <sup>12</sup>Tadmor, G., Bissex, D., Noack, B. R., Morzyński, M., Colonius, T., and Taira, K., “A Fast Approximated POD Algorithm for Long Time Data Trajectories,” *4th Flow Control Conference 4th Flow Control Conference 38th AIAA Fluid Dynamics Conference and Exhibit*, 2008, Submitted.
- <sup>13</sup>Boashash, B., “Estimating and interpreting the instantaneous frequency of a signal. I. Fundamentals,” *Proc. IEEE*, Vol. 80, 1992, pp. 520–538.
- <sup>14</sup>Boashash, B., “Estimating and interpreting the instantaneous frequency of a signal. II. Algorithms and applications,” *Proc. IEEE*, Vol. 80, 1992, pp. 540–568.
- <sup>15</sup>Luchtenburg, M., Tadmor, G., Lehmann, O., Noack, B. R., King, R., and Morzynski, M., “Tuned POD Galerkin models for transient feedback regulation of the cylinder wake,” *44th AIAA Aerospace Sciences Meeting and Exhibit*, 2006, Paper AIAA-2006-1407.
- <sup>16</sup>Morzyński, M., Stankiewicz, W., Noack, B. R., King, R., Thiele, F., and Tadmor, G., “Continuous mode interpolation for control-oriented models of fluid flow,” *Active Flow Control*, edited by R. King, Vol. 95 of *Notes on Numerical Fluid Mechanics and Multidisciplinary Design*, Springer Verlag, Berlin, Germany, 2007, pp. 260–278.
- <sup>17</sup>Stuart, J., “On the non-linear mechanics of hydrodynamic stability,” *J. Fluid Mech.*, Vol. 4, 1958, pp. 1–21.
- <sup>18</sup>Dušek, J., Le Gal, P., and Fraunie, P., “A numerical and theoretical study of the first Hopf bifurcation in a cylinder wake,” *J. Fluid Mech.*, Vol. 264, 1994, pp. 59–80.
- <sup>19</sup>Zielinska, B. and Wesfreid, J., “On the spatial structure of global modes in the wake flow,” *Physics of Fluids*, 1995, pp. 1418 – 1424.
- <sup>20</sup>Siegel, S., Cohen, K., and McLaughlin, T., “Feedback Control of a Circular Cylinder Wake in Experiment and Simulation,” *33rd AIAA Fluids Conference and Exhibit*, Orlando, Florida, U.S.A., June 23–26, 2003, 2003, Paper No 2003-3571.

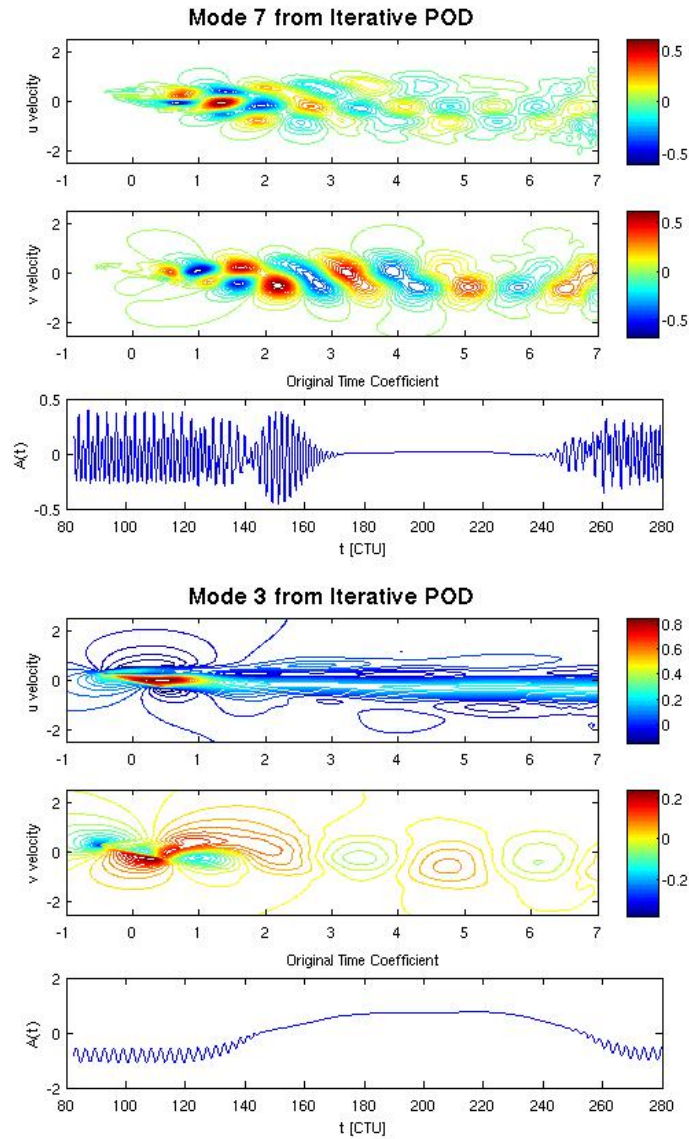


Figure 2. Modes produced by the approximate POD algorithm. In each triad, top and middle: level curves of the stream-wise and transverse velocity components; bottom: time trace of the Fourier coefficient of these modes. The latter clearly illustrates the mixing of multiple temporal harmonics, reflecting the blending of coherent flow structures at different wave lengths.

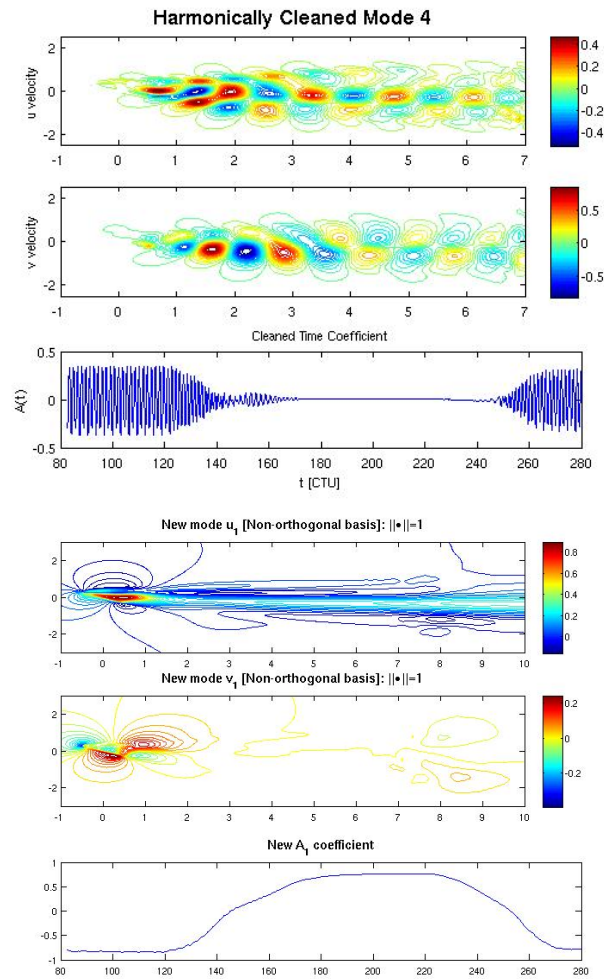


Figure 3. Harmonically cleaned counterparts of the modes in Figure 2. In each triad, top and middle: level curves of the stream-wise and transverse velocity components, featuring a clear dominance of a single wave length (top triad) and no periodic structures in a mean field correction mode (bottom triad); bottom: single frequency and slowly varying time traces of the Fourier coefficients of these modes.